

Effect of Artificially Produced Pit-Like Defects on the Fatigue Life (S-N Curve) of AISI 410 Stainless Steel Compressor Blades Material

M. Mat Noh^{1,a}, M. A. Khattak^{*1}, M. N. Tamin^{1,b}, M. S. Khan^{1,c}, N. Iqbal^{2,d}, M. S. E. Kosnan^{3,e},
S. Kazi^{4,f}, M. Khan^{5,g}, T. Subhani^{5,h} and M. Anwar^{6,i}

¹Department of Applied Mechanics and Design, Faculty of Mechanical Engineering, Universiti Teknologi Malaysia, (UTM), Johor, Malaysia.

²Medical Devices & Technology Group (MEDITEG), Faculty of Biosciences and Medical Engineering, Universiti Teknologi Malaysia, 81310 Johor Bahru, Johor, Malaysia.

³Department of Facilities Maintenance Engineering, Universiti Kuala Lumpur Malaysia Institute Of Industrial Technology, 81750 Johor, Malaysia.

⁴Department of Mechanical Engineering, The Islamic University Madinah, P.O. Box 170 Madinah, 41411, Saudi Arabia.

⁵Department of Materials Science and Engineering, Institute of Space Technology, 44000, Islamabad, Pakistan.

⁶Faculty of Engineering and Science, Curtin University, Sarawak Campus, 98009 Miri, Sarawak, Malaysia.

*muhdadil@utm.my, a mazmir.mn@gmail.com, b taminmn@fkm.utm.my, c engrsalman091@gmail.com,
d nidaiqbal@biomedical.utm.my, e mshahruleffendy@unikl.edu.my, f skazi@iu.edu.sa,
g mahmoodkhan77@yahoo.com, h tayyab.subhani@ist.edu.pk, i mahmood.a@curtin.edu.my

Abstract – *In this research work, an experimental investigation was conducted to explore the effects of artificially produced pit-like defects on the fatigue life of the members made of AISI 410 martensitic stainless steel. Compressor blades in power generating industries, made of AISI 410 stainless steel, commonly suffer from pitting corrosion. Evolution in microstructure properties and chemical composition of the material has been investigated. The structure reveals matrix of equiaxed ferrite grains, with randomly dispersed particles of chromium carbide. Well defined pit-like defects were artificially produced on various specimen and fatigue tests were conducted to acquire the stress-life (S-N) properties of the material. Resulted stress-life (S-N) curves showed that the fatigue life of the specimens with larger dimensions (diameter and depth) of artificial pits were lower than the specimens with smaller size of artificial pit. However, even the smaller pit size can lead to early failure of the specimen and can reduce the fatigue life by approximately 13.6% from the original specimen without pit. Copyright © 2016 Penerbit Akademia Baru - All rights reserved*

Keywords: AISI 410 Steel, Compressor Blades, Pitting Corrosion, stress-life (S-N) curves.

1.0 INTRODUCTION

Compressors are one of the main components in gas turbine used in power generating industries. Fatigue failure originating from pitting corrosion has been identified as one of the dominant life-limiting factors for the gas turbine blades [1-8]. In power generating industries, the gas turbine blades are subjected to the corrosive environment from the incoming air during the operation and can result in the formation of pitting corrosion on the surface of the blades [9-12]. There have been several studies in the literature reporting that when they operate in centrifugal and vibratory loading conditions, the cyclic loading and unloading during operation coupled with the presence of pitting corrosion much reduce the life of the compressor blades [13]. In this respect, the effect of pitting corrosion on the fatigue life of the compressor blades need to be established.

Pitting corrosion can have a detrimental influence on the strength and fatigue life of the material where it acts as stress concentration sites and raise the stress level locally, facilitating fatigue crack initiation and propagation, leading to final fracture of the blades [10, 13]. Nakai et al. [14] from his research summarized that the nominal tensile strength of pitted structural members decreases gradually while the total elongation decreases drastically with the increase of thickness loss due to pitting. Yoshino and Ikegaya [15] performed experimental investigations on 12Cr-Ni-Mo martensitic stainless steel in chloride and sulphide environments and observed that even small amount of H₂S have a significant detrimental effect on the resistance of the steels to the pitting corrosion.

Many researchers have argued that the geometric discontinuity due to a pit induces a large stress gradient with high magnitude of localized stress [16-18]. The time to nucleate a corrosion pit under surface straining was analysed at the microscale [19]. A relationship between surface stress and pitting corrosion has also been established [20]. The effect of pitting damage is to reduce the life of structural components [21-26]. The study by Becker et al. [27] analyzed the effect of pitting corrosion on fatigue and fracture behaviour of 13% Cr stainless steel and highlighted the interactive effects of corrosion pit nucleation and growth. Fatigue cracks have initiated from the pits on the leading edge and propagated during service operation and led to the failure of the blade [13, 28].

Earlier research has already established the pits geometry details and its effect on the strength of the material [29]. This research examines the fatigue life (S-N curves) of AISI 410 martensitic stainless steel compressor blade material with different geometries of artificially produced pit-like defects. Several cases using the same specimen geometry but different artificial pit geometries has been examined. The fatigue life of the stainless steel sample coupons with and without artificial pit are compared.

2.0 EXPERIMENTAL DETAILS

2.1 Material

The material employed in this study is an AISI 410 martensitic stainless steel which was received in the form of circular plate with radius and thickness of 440 mm and 18 mm, respectively. It was wire-cut using Electrical Discharge Machine (EDM) into dog-bone shaped specimen to be used for fatigue testing. Figure 1 illustrates the dimension details of the dog-bone shaped specimen with a gage length of 25 mm.

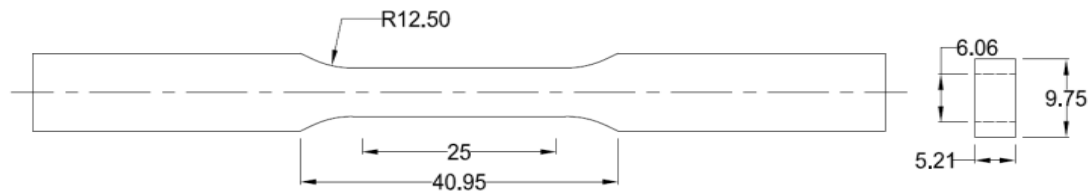


Figure 1: Geometry of dog-bone shaped specimen (dimensions in mm)

The chemical composition of the material was established using Glow Discharge Spectrometry (GDS) machine and is shown in Table 1. The primary alloying elements are chromium (Cr) and carbon (C). AISI 410 martensitic stainless steel have higher amount of carbon and chromium to obtain high strength, high toughness and good corrosion resistance while manganese and nickel contribute to improved toughness of the steel. Generally, the chromium and carbon content for martensitic stainless steel lies between 0.08 – 1.10 % for carbon and 12 – 18 % for chromium [30]. Results obtained from GDS for the selected material revealed that the carbon and chromium content are 0.15 and 14.2 %, respectively. To obtain the mechanical properties of the respective material as shown in Table 2, tensile test was performed on the dog bone shaped specimen.

Table 1: Chemical composition (in weight percent) of AISI 410 stainless steel

Material	C	Mn	P	S	Si	Cr	Ni	Mo	Al	V	Fe
AISI 410	0.2	0.5	0.02	0.002	0.35	14.20	0.39	0.01	0.003	0.03	Bal.

Table 2: Mechanical properties of AISI 410 steel at room temperature

Material	Tensile Strength (MPa)	Yield Strength (MPa)	Elongation (pct.)	Maximum Load (kN)
AISI 410	656.04	620.17	30	21.27

2.2 Microstructure

For microstructural study, the material was observed at three orthogonal section planes. The microstructural observations were obtained and the images of the microstructure at different magnification were captured using Optical Microscope equipped with image analyser. For sample preparation, the specimens were finely grind, polished and etched in the etching solution (5 ml HCL + 2gr Picric acid + 100 ml Ethyl alcohol) for approximately 7 seconds.

Figure 2 shows microstructures of the AISI 410 martensitic stainless steels at the three different orthogonal section planes. The microstructure shows a typical body-centered tetragonal (bct)

structure. The dark area represents martensitic phase while light area shows the ferrite phase. The structure reveals the matrix of equiaxed ferrite grains, with randomly dispersed particles of chromium carbide. Since qualitatively identical microstructure is displayed for each section, the material is expected to behave in isotropic manner.

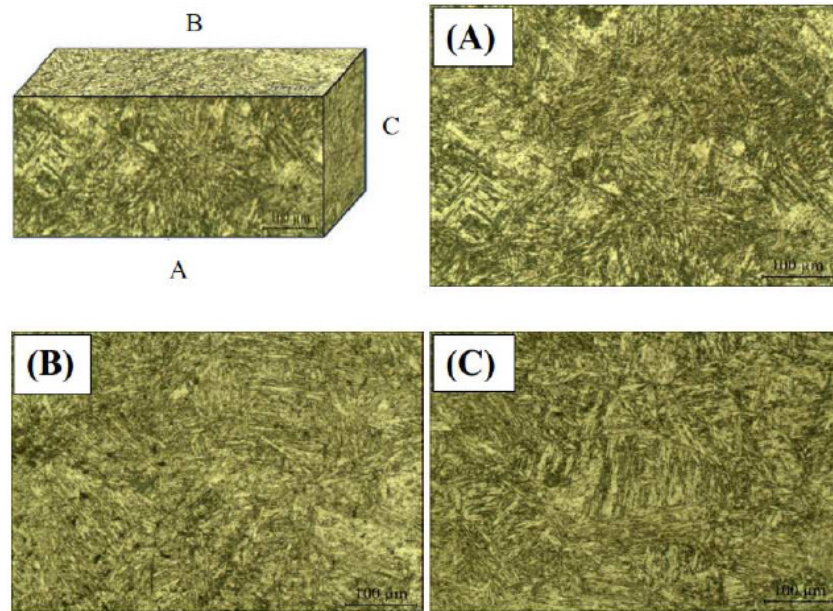


Figure 2: Microstructure observations for section A, B and C

2.3 Artificial Pit Formation on Specimen

During previous research works, pitting corrosion experiment has been performed according to ASTM G48-11 standard to quantify the specimen immersion time for creating the desired characteristic corrosion pit morphology [31]. Pit geometries from the corroded specimens were quantified and compared with the measured geometry details of the pitted retired blades from Sultan Iskandar Power Generating Plant, Johor, Malaysia. Approximately 300 pits produced on the specimen were measured for their diameters and depths. Based on the analysis, the maximum, minimum and nominal pit diameter and depth values are listed in Table 3.

Table 3: Pit geometry details

	Pit Diameter (mm)	Pit Depth (mm)
Maximum	1.00	0.75
Minimum	0.30	0.30
Nominal	0.50	0.50

Artificial pits were then produced on the surface of the dog-bone shaped specimen using Sinker EDM machine. Four cases of artificial pit were used in this study. The diameter and depth for

all cases are shown in Table 4 and the specimen with artificially produced pit is shown in Figure 3.

Table 4: Geometry details of Case 1 – Case 4

Case	Pit Diameter	Pit Depth
1	Maximum (1.00 mm)	Maximum (0.75 mm)
2	Maximum (1.00 mm)	Minimum (0.30 mm)
3	Minimum (0.30 mm)	Maximum (0.75 mm)
4	Minimum (0.30 mm)	Minimum (0.30 mm)

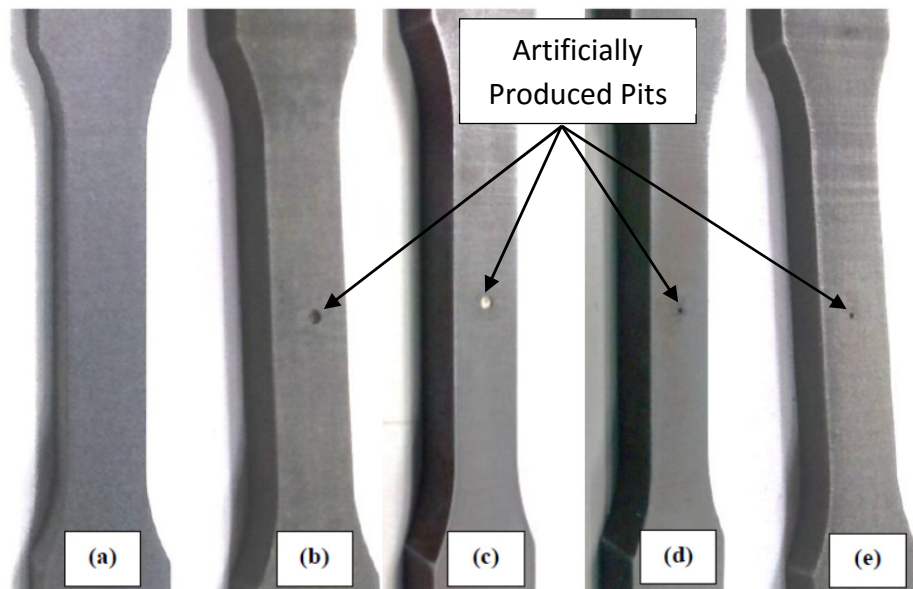


Figure 3: Dog-bone shaped specimens with artificial pit for (a) as-received (without pit), (b) Case 1, (c) Case 2, (d) Case 3, and (e) Case 4

3.0 RESULTS AND DISCUSSION

Fatigue test were performed to all of the specimens in order to generate the stress-life (S-N) curves. There are five types of specimens used in this experiment which are as-received and specimens with artificial pit (Case 1 – Case 4). The results of the tests were analysed and compared to one another. All tests were performed using servo-hydraulic Universal Testing Machine at room temperature with stress ratio of 0.1 and frequency of 20 Hz. The S-N curves for all cases of AISI 410 martensitic stainless steel specimens are shown in Figure 4.

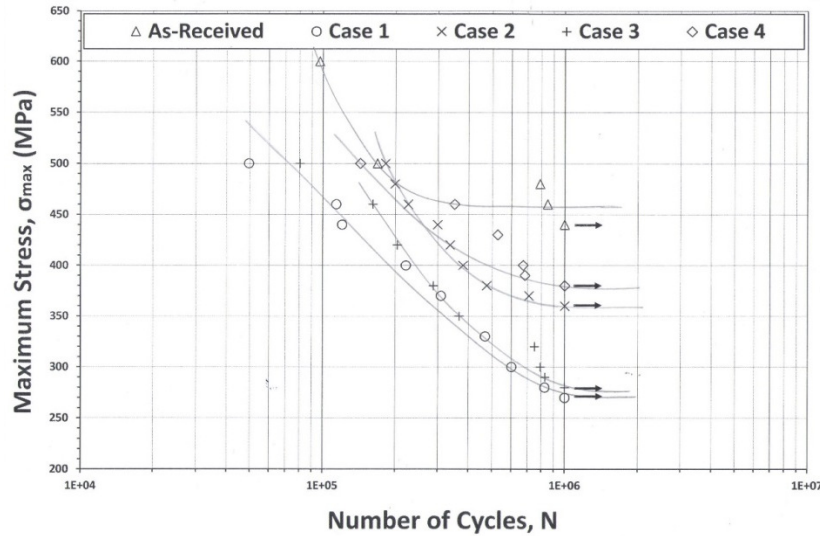


Figure 4: Stress-life (S-N) curves for as-received and all cases with artificial pit

The arrow on the graph indicates the infinite life of the specimen for a given loading. From the graph, fatigue limit σ_{max} of the specimen decrease with the increase of artificial pit size (either pit depth or diameter). As-received specimen having the highest fatigue life amongst all cases since this specimen have no pit. From all cases with artificial pit, the lowest fatigue life is for Case 1, followed by Case 3, Case 2 and Case 4.

Case 1 have the lowest fatigue life because the size of the pit on that specimen is the largest (maximum diameter, maximum depth). This is followed by Case 3 which having the minimum diameter and maximum depth of the pit size. The fatigue life of Case 3 is lower than Case 2 and Case 4 because of the depth size which is maximum. Even though the pit diameter is minimum, the maximum depth of the pit affect and reduce the fatigue life. Then, it is followed by Case 2 which having the maximum diameter and minimum depth. Finally, Case 4 having the longest fatigue life amongst all the case with artificial pit since it have both minimum size for pit diameter and depth.

4.0 CONCLUSIONS

From this study, it can be concluded that the fatigue life of the specimen with artificial pit is lower than as-received specimen. The lowest fatigue life is possessed by Case 1, followed by Case 3, Case 2 and Case 4. The depth of the pit plays an important role in reducing the fatigue life of the specimen. The deeper the depth of the pit, the lower the fatigue life. Even the smaller pit size can lead to early failure of the specimen. This is proven when the fatigue life of Case 4 (minimum diameter, minimum depth) has been reduced by approximately 13.6 % from the as-received specimen even it have the minimum size of diameter and depth.

ACKNOWLEDGEMENT

This project is supported by the Ministry of Science, Technology and Innovation (MOSTI), Government of Malaysia, Project No. 4F156.

REFERENCES

- [1] D. Linden, Long Term Operating Experience with Corrosion Control in Industrial Axial Flow Compressors, Proceedings of the Fortieth Turbomachinery Symposium, September 12-15 (2011) Houston, Texas
- [2] Y. Zhang, D. D. Macdonald, M. Urquidi-Macdonald, G. R. Engelhardt, R. B. Dooley, Passivity breakdown on AISI Type 403 stainless steel in chloride-containing borate buffer solution, Corrosion science 48 (2006) 3812-3823.
- [3] S. Zhou, A. Turnbull, Overview Steam turbines: Part 1—Operating conditions and impurities in condensates, liquid films and deposits, Corrosion Engineering, Science and Technology 38 (2003) 97-111.
- [4] O. Jonas, J.M. Mancini, Steam turbine problems and their field monitoring, Materials performance 40 (2001) 48-53.
- [5] B. M. Schönbauer, S. E. Stanzl-Tschegg, A. Perlega, R. N. Salzman, N. F. Rieger, A. Turnbull, S. Zhou, M. Lukaszewicz, D. Gandy, The influence of corrosion pits on the fatigue life of 17-4PH steam turbine blade steel, Engineering Fracture Mechanics 147 (2015) 158-175.
- [6] J. Bhandari, F. Khan, R. Abbassi, V. Garaniya, R. Ojeda, Modelling of pitting corrosion in marine and offshore steel structures—A technical review, Journal of Loss Prevention in the Process Industries 37 (2015) 39-62.
- [7] L. Witek, M. Wierzbińska, A. Poznańska, Fracture analysis of compressor blade of a helicopter engine, Engineering Failure Analysis 16 (2009) 1616-1622.
- [8] G.S. Chen, K.-C. Wana, M. Gao, R.P. Wei, T.H. Flournoy, Transition from pitting to fatigue crack growth—modeling of corrosion fatigue crack nucleation in a 2024-T3 aluminum alloy, Materials Science and Engineering: A 219 (1996) 126-132.
- [9] D.A. Horner, B.J. Connolly, S. Zhou, L. Crocker, A. Turnbull, Novel images of the evolution of stress corrosion cracks from corrosion pits, Corrosion Science 53(2011) 3466-3485.
- [10] M. Jahangiri, A. Fallah, A. Ghiasipour, Cement kiln dust induced corrosion fatigue damage of gas turbine compressor blades—A failure analysis, Materials & Design 62 (2014) 288-295.
- [11] J.R. Laguna-Camacho, L.Y. Villagrán-Villegas, H. Martínez-García, G. Juárez-Morales, M.I. Cruz-Orduña, M. Vite-Torres, L. Ríos-Velasco, I. Hernández-Romero, A study of the wear damage on gas turbine blades, Engineering Failure Analysis, (2015) Article in Press.
- [12] E. Poursaeidi, A. Babaei, F. Behrouzshad, M.R. Mohammadi Arhani, Failure analysis of an axial compressor first row rotating blades, Engineering Failure Analysis 28 (2013) 25-33.
- [13] A. Mokaberi, R. Derakhshandeh-Haghighi, Y. Abbaszadeh, Fatigue fracture analysis of gas turbine compressor blades, Engineering Failure Analysis 58 (2015) 1-7.
- [14] T. Nakai, H. Matsushita, N. Yamamoto, H. Arai, Effect of pitting corrosion on local strength of hold frames of bulk carriers (1st report), Marine structures 17 (2004) 403-432.

- [15] Y. Yoshino, A. Ikegaya, Pitting and Stress Cracking of 12Cr-Ni-Mo Martensitic Stainless Steels in Chloride and Sulfide Environments, *Corrosion* 41 (1985) 105-113.
- [16] M. Cerit, Numerical investigation on torsional stress concentration factor at the semi elliptical corrosion pit, *Corrosion Science* 67 (2013) 225-232.
- [17] Z. T. Mu, D. H. Chen, Z. T. Zhu, B. Ye, The Stress Concentration Factor of Different Corrosion Pits Shape, *Advanced Materials Research* 152-153 (2011) 1115-1119.
- [18] A. Turnbull, L. Wright, L. Crocker, New insight into the pit-to-crack transition from finite element analysis of the stress and strain distribution around a corrosion pit, *Corrosion Science* 52 (2010) 1492-1498.
- [19] V. Vignal, N. Mary, C. Valot, R. Oltra, L. Coudreuse, Influence of elastic deformation on initiation of pits on duplex stainless steels, *Electrochemical and solid-state letters* 7(2004) C39-C42.
- [20] R. Oltra, V. Vignal, Recent advances in local probe techniques in corrosion research—analysis of the role of stress on pitting sensitivity, *Corrosion science* 49 (2007) 158-165.
- [21] J. Tousek, Theoretical aspects of the localized corrosion of metals, *Materials Science Surveys* 3 (1985) 180.
- [22] J. Rajasankar, N.R. Iyer, A probability-based model for growth of corrosion pits in aluminium alloys, *Engineering Fracture Mechanics* 73 (2006) 553-570.
- [23] H.C. Wu, B. Yang, Y.Z. Shi, Q. Gao, Y.Q. Wang, Crack Initiation Mechanism of Z3CN20. 09M Duplex Stainless Steel during Corrosion Fatigue in Water and Air at 290° C, *Journal of Materials Science & Technology* 31 (2015) 1144-1150.
- [24] S.H. Xu, Estimating the effects of corrosion pits on the fatigue life of steel plate based on the 3D profile, *International Journal of Fatigue* 72 (2015) 27-41.
- [25] A. Shekhter, B.R. Crawford, C. Loader, W. Hu, The effect of pitting corrosion on the safe-life prediction of the royal australian air force P-3C Orion Aircraft, *Engineering Failure Analysis* 55 (2015) 193–207.
- [26] I. Fernandez, J.M. Bairán, A.R. Marí, Corrosion effects on the mechanical properties of reinforcing steel bars. Fatigue and σ - ϵ behavior, *Construction and Building Materials* 101 (2015) 772-783.
- [27] K. Becker, A. Rukwied, The effect of surface degradation on fatigue and fracture behaviour, *Materials & Design* 14 (1993) 175-182.
- [28] S.D. Kumari, Satyanarayana, and M. Srinivas, Failure analysis of gas turbine rotor blades, *Engineering Failure Analysis* 45 (2014) 234-244.
- [29] M. Mat Noh, F. Mozafari, M. A. Khattak, M. N. Tamin, Effect of Pitting Corrosion on Strength of AISI 410 Stainless Steel Compressor Blades, *Applied Mechanics and Materials* 606 (2014) 227-231.
- [30] F.S. Merritt, J.T. Ricketts, *Building design and construction handbook* 13 (2001) Citeseer.